Current Redistribution in a Superconducting Multi-Strand 35 kA DC Cable Demonstrator

M. J. Wolf, W. H. Fietz, *Senior Member, IEEE,* M. Heiduk, C. Lange, and K.-P. Weiss

***Abstract*— High temperature superconductors (HTS) are discussed as energy-efficient solutions for industrial high-current applications beyond 10 kA e.g. bus bar systems in industrial electrolysis plants. In this contribution, the experimental test of a 3.6-meter-long 35 kA DC demonstrator, made from twelve high-current HTS CrossConductor (HTS CroCo) strands in an liquid nitrogen bath at T = 77 K is presented. In this work, a common connector concept of the twelve HTS CroCo strands is proposed. Compared to earlier results without common connector, lead resistances were effectively reduced and current distribution among the individual strands was significantly facilitated. This is confirmed by the observation of increased critical cable current of 37.6 kA compared to 33 kA in previous work without low-resistive common connector. Additionally, the current range, in which all twelve strands reached their critical electric field, was found to be reduced from >7 kA to 2 kA. Results are discussed and assessed with the help of an electric circuit model, from which the solder resistances at the connections could be obtained by fitting.**

Particular focus was given to the investigation of current redistribution in the demonstrator. Therefore, a heater was installed on one HTS CroCo strand, and activated to raise the temperature on this strand and quench a single strand locally. It is observed that current is redistributed through the common connectors to the other strands.

***Index Terms*—Current Redistribution, DC power distribution, HTS Cable, HTS CroCo, REBCO**

I. Introduction

ALUMINUM electrolysis uses highest direct currents (DC) up to 600 kA in modern production plants [1] [2]. The quasi-continuous operation at stable operating conditions of such plants, low voltages of approx. 1-2 kV and the limited circuit length (few km at maximum in total) make these systems interesting for applications of a high-temperature superconducting (HTS) busbar or cable solution [3]. In combination, there is a high potential for substantial energy savings using superconducting instead of conventional Aluminum busbar solutions as it was already recognized in 1995 [3]. Generally, two different DC circuits are used in Aluminum electrolysis and HTS could be used in both. The main circuit is connecting the individual cells (which are typically arranged in a U-shape) to the rectifier. Here the distance from the rectifier to the first cell or between the two lines are of particular interest, as the distance between individual cells is too small.

M. J. Wolf, (e-mail: Michael.Wolf@kit.edu). W. H. Fietz, M. Heiduk, C. Lange, and K.-P. Weiss are with the Institute for Technical Physics (ITEP), Karlsruhe Institute of Technology (KIT), 76344 Eggenstein-Leopoldshafen, Germany

Color versions of one or more of the figures in this paper are available online at http://ieeexplore.ieee.org.

Digital Object Identifier will be inserted here upon acceptance.

Additionally, a secondary circuit (of not necessarily the same amperage) is used for the compensation of magnetic fields and could be built using HTS as well [2] [3]. As the major source of losses in such a HTS high-direct-current cable is due to the current leads connecting the superconductor to ambient temperature.

Recently, a multi-stage cooled current lead for industrial high DC applications was developed and tested [4].

Up to now, several HTS DC demonstrators or prototype installations with currents of ≥10 kA were realized, e.g. a 10 kA and 360 m long cable in an Aluminum electrolysis plant [5], a 10 kA cable for railway systems [6], for 20 kA and 25 m length for an electrolysis plant in Germany [7], and a 35 kA and 3.6 m long demonstrator and test setup for research on high current cables at KIT [8], [9] [10] [11].

This work shows important application-relevant improvements of the aforementioned 35 kA demonstrator at KIT, which is built from twelve so-called HTS CroCo high current HTS strands connected in parallel. Fig. 1(a) shows the configuration of previous work. There, all HTS CroCo strands (black) were connected individually through copper litz wires (diagonal stripes) to terminals (solid grey). This way of connection proved effective to characterize all twelve strands individually [9] and to measure the individual currents in each strand directly [11] but did not allow to investigate current redistribution due to the large series resistance of ~ 8 μΩ per strand and the related high voltage drop of ~ 24 mV at I = 3kA along the leads compared to the superconductor, even at the superconductor's critical current $V(I_c)$ = 0.36 mV for an electric field criterion E_c = 1 μV/cm, and demonstrator length L = 3.6 m. Therefore, a common connector was designed and installed at the HTS CroCo ends, such that only the unavoidable soldered connections from the common connector to the superconducting strands act as series resistances. From previous work [11], these resistances are expected to be in the range of ~0.2 μΩ only, which means a reduction by 97.5 % compared to the previous configuration. Consequently, the voltages of the leads and along the superconductor are of the same order of magnitude at the critical current. Fig. 1(b) shows the new configuration (for two strands only) with common connectors shown as checkerboard patterns.

Current redistribution effects were studied experimentally for insulated, multi-strand NbTi [12] wires and modelled with the help of RL circuits [13] as non-equal currents in different strands of a multi-strand superconductor reduces the critical current in particular for high current ramp rates [14] and are therefore of interest for rapidly ramped magnets.

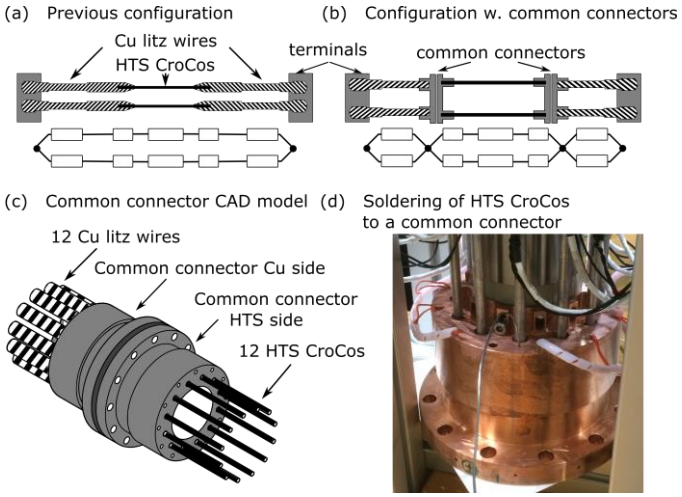

Fig. 1 (a) Connection scheme of the twelve HTS CroCos used in previous studies. All HTS CroCos (black) are connected individually by Cu litz wires (diagonal stripes) with a lead resistance of ~ 8μΩ. (b) New configuration investigated in this work. Common connectors (grey) are introduced immediately at the ends of the HTS CroCo strands to minimize the effective lead resistances and allow for current redistribution. On one of the twelve strands, a heater is installed locally at the center of the strand. (c) Simplified CAD model of the novel common connector. The connector is separable at its base plate (dark grey) to facilitate the installation. (d) (color online) Photograph of the common connector during soldering of the HTS CroCos.

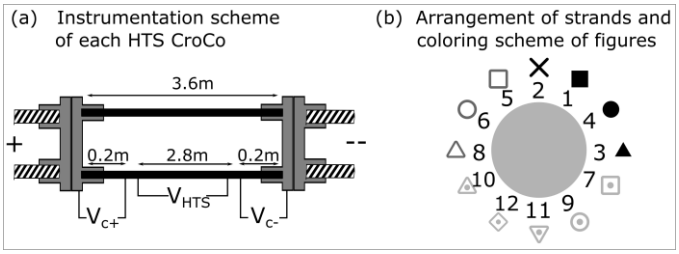

Fig. 2. (a) Instrumentation scheme of the demonstrator. For clarity only two (out of twelve) HTS CroCos are shown. Voltages are measured on the mid-sections of the HTS CroCo superconductor V_{HTS} over a length of 2.8 m and on both connections to the common connector (V_{c+}, V_{c-}). Note that the connectors include not only the contact resistance but also 0.2 m of superconductor. (b) Arrangement of the HTS and symbols representing each HTS CroCos in the following graphs. Note that a heater is installed on HTS CroCo #2 (black cross). The neighboring HTS CroCos are denoted to one side of #2 by filled black symbols (#1,#4,#3) and to the other side by open grey symbols (#5, #6, #8). The type of symbol characterizes the distance to HTS CroCo # 2. The five HTS CroCos furthest away from #2 (#7, #9, - #12) are represented by light grey symbols.

II. The 35 kA Demonstrator with Common Connectors

Fig. 1(c) shows a simplified model of the novel common connector. The connector is separable at a central base plate to facilitate the installation of the demonstrator into the test facility. The twelve HTS CroCos are soldered to the common connector over a length of 10 cm using $In_{52}Sn_{48}$ solder with a melting temperature of 118 °C, sufficiently below the melting temperature of the HTS CroCos, to prevent a re-melting of the $Sn_{63}Pb_{37}$ solder used in the fabrication of the HTS CroCos. The solder process is performed in an upright position using cartridge heaters (Fig. 1(d)).

For the evaluation of the demonstrator, each of the HTS CroCos is equipped with three pairs of voltage taps that record the voltages on the mid-sections of all HTS CroCo superconductor V_{HTS} over a length of 2.8 m and on both connections to the base plates of the common connector (V_{c+}, V_{c-}). Note that the connectors include not only the contact resistance but also the voltage originating from 0.2 m of superconductor. A 12-channel quench detection system is monitoring the voltages of all twelve HTS CroCos individually. Fig. 2(a) shows the schematics of the instrumentation, for clarity, only two strands are shown. The twelve HTS CroCos are arranged in a circular arrangement on a carrier of diameter of 110 mm. Fig. 2(b) shows the (not-to-scale) cross-sectional arrangement of the HTS CroCos and the symbols representing each HTS CroCo in the following graphs. Note that a foil heater is installed locally over few cm length on HTS CroCo #2 (black cross) which is activated to quench this strand locally and initiate the redistribution process, similar to another work on current redistribution in HTS cables [15]. The neighboring HTS CroCos are denoted to one side of #2 by filled black symbols (#1,#4,#3) and to the other side by open grey symbols (#5, #6, #8). The type of symbol (square, circle, triangle) characterizes for both sides the distance to HTS CroCo # 2. The five HTS CroCos furthest away from #2 (#7, #9 - #12) are represented by light grey symbols.

III. Electric Model of the Demonstrator

The demonstrator is modeled by an electric model using linear (Ohmic) resistances $V(I) = R \cdot I$ for non-superocnducting parts and a power-law dependence of the superconducting parts of the cable $V(I) = E_c \cdot L \cdot (I/I_c)^n$, where $E_c = 1\mu V/cm$ denotes the electric field criterion for determination of I_c, L is the length, I_c is the critical current and n the exponent of the power law dependence. The base plate of the common connector is assumed to be an equipotential, such that the sum of both connections and along the superconductor must be the same for all twelve strands. The measured connector voltages V_{c+} and V_{c-} are modeled as a sum of a linear part for the soldered connection and the current path in the copper and a superconducting part with L = 0.2 m (see Fig. 2(a)). The voltages along the HTS CroCos are described by the power law dependence, for HTS CroCo #2 a linear contribution is added if the heater is activated. Each HTS CroCo is assumed to be homogeneous along its length, i.e., described by a single $I_{c,i}$ value, and resistances of the soldered connections are assumed to be independent of current. Detailed self-consistent calculations of the critical currents in cable-field and self-field condition show that for the given configuration the field at the location of the superconductor is dominated by the field of the HTS CroCo itself [10] due to the separation between the strands (see Fig. 2(d)). Therefore, the CroCos are characterized by their self-field critical currents from [9], with a constant correction factor of 0.96 to match with the measured cable critical current, accounting for slight cable-field effects or minor degradations during preparation of the new demonstrator. The n-value is assumed to be 25 for all HTS CroCos.

The measured voltage data along the mid-superconducting part of the cable (2.8 m) V_{HTS} and the sum of the voltages at both

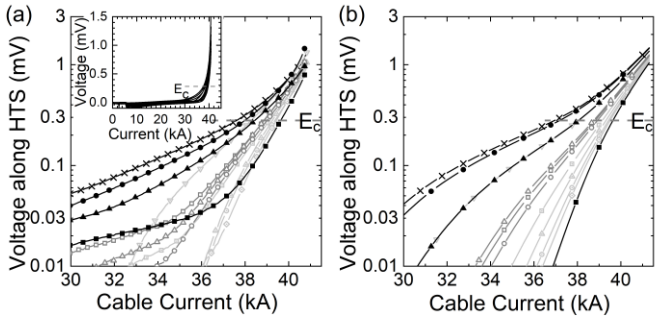

Fig. 3. Performance of the demonstrator at a constant cable current ramp with ramp rate of 100 A/s. (a) Voltage along the mid-sections of the superconducting part of the cable (see Fig. 2(b) for the symbol convention) over a length of 2.8 m. The main panel shows the voltages of the twelve HTS CroCos in a semi-logarithmic representations for cable currents ≥30 kA. The inset shows the same data in a linear representation over the whole current range. (b) Calculated voltage profiles along the mid-sections of the superconducting part of the cable.

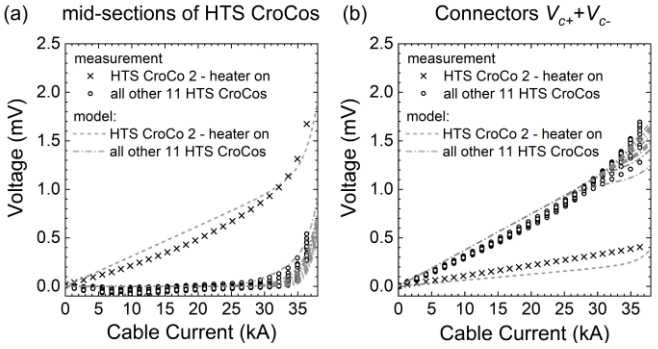

Fig. 4. Performance of the demonstrator with permanently activated heater on HTS CroCo #2. This strand is represented by a black cross, all other eleven HTS CroCos are not distinguished for clarity of the plots. The dashed and dash-dotted grey lines are calculations according to the electric circuit model. (a) Voltage along the mid-sections of the superconducting part of the cable as function of the cable current. (b) Sum of the connector voltages (V_{c+}+V_{c-}) during the same current ramp.

connections, $V_c = V_{c+} + V_{c-}$, is then fitted to the model by adjusting the soldered contact resistances $R_{c,i}$ of all 12 HTS CroCos in the following way: First, the total voltage including terminals is calculated according to $V_{total} = V_{HTS} \cdot 3.2/2.8 + V_c$. It is averaged over all 12 CroCos and interpolated on equidistant cable current steps of 200 A. For a given voltage V_0, the individual currents in each of the 12 strands are calculated and added to obtain the total cable current. The measured voltages of all the mid-sections of all 12 HTS CroCos, $V_{HTS,i}(I_{cable})$ and $V_{c,i}(I_{cable})$, are compared to the calculated ones at the interpolated cable current steps. By varying the contact resistances $R_{c,i}$ and minimizing the sum of squared residuals of $V_{HTS,i} + V_{c,i}$, the best fit to the data is obtained.

IV. Results of Cable Current Ramps

Fig. 3(a) shows the voltage along the mid-sections of the superconducting HTS CroCos (see Fig. 2(b) for the symbol convention) over a length of 2.8 m during a cable current ramp with dI_{cable}/dt = 100A/s. The main panel shows the voltages of the twelve mid-sections of the HTS CroCos in a semi-logarithmic representation for cable currents of more than 30 kA. The inset shows the same data in a linear representation over the whole current range. The grey horizontal line indicates in both panels the electric field criterion for the determination of the critical current. The criterion is reached first for HTS CroCo #2 at a cable current of 37.6 kA and last for HTS CroCo #1 at 39.6 kA. The narrow critical current scattering of 2 kA indicates good current distribution and similar contact resistances in the common connector. In previous work without common connector (configuration of Fig. 1(a)), the critical current scattering was >7 kA [11]. Fig. 3(b) shows the fitted voltage profiles along the mid-sections of the HTS CroCos. The connector resistances of the twelve HTS CroCos (sum of + and – connector) were determined by fitting and range from 325 nΩ to 548 nΩ, in agreement with expectation of about 400 nΩ.

In a subsequent test, the cable current was again ramped with 100 A/s but now the heater on HTS CroCo # 2 was permanently activated at a heater current I_{heater} = 1.0 A corresponding to P_{heater} = 56 W. Fig. 4(a) shows the voltage along the mid-sections of the superconductor and Fig. 4(b) presents the sum of the positive and negative connector voltages as function of the cable current. HTS CroCo #2 (with heater) is represented by a black cross, all other eleven HTS CroCos (without heaters) are not distinguished for clarity of the plots. HTS CroCo #2 shows a non-zero voltage over the whole current range indicative of a local normal zone at the heated length.

The dashed and dash-dotted grey lines are calculations according to the electric circuit model with same parameters as in the ramp without heating (Fig. 3(b)) apart from an additional linear resistance added in series to the superconductor in HTS CroCo #2 to account for the normal zone generated by the heater. As the total voltage along all HTS CroCos including the connections must be equal, the non-zero voltage along the superconductor requires a smaller voltage along the connectors. This is observed and shown in Fig. 4(b). If one assumes the soldered resistances to be independent of the current, the voltage along the termination is an indicator of the current. HTS CroCo #2 carries consequently less current and the onset of the superconducting transition occurs at a lower cable current of ~ 35 kA with heater (compared to 37.6 kA without heater). The data is fitted to the circuit model assuming that only a single linear resistor with $R_{2,H}$ = 1.8 μΩ is added in series with the power-law superconductor to $V_{HTS,2}$. All other parameters are the same as for the measurement without heating of HTS CroCo #2.

V. Current Redistribution

In order to analyze current redistribution effects in detail, the response of the demonstrator to heating pulses at constant cable current is investigated.

The left column of subfigures in Fig. 5 shows the voltage responses of the different parts of the demonstrator (negative (a) / positive (c) connector and mid-sections of the superconductor (e)) to heating pulses I_{heater} = 0.9 A on HTS CroCo #2 at constant cable current of I_{cable} = 25 kA. For better comparability between the 12 HTS CroCos, the voltages of the connectors are

normalized to their values before heater activation, i.e. $V_{norm} = V_c(t) / V_c(t<0)$.

The heater was activated at t = 0 and deactivated at t = 58.5 s as indicated by vertical dashed lines. The time since heater activation is plot on the horizontal axis. Note that it is split for all plots between 25 s and 55 s as denoted by the grey bar and that the vertical axis of (e) is split as denoted by the grey bar with different scales for the two parts. The five HTS CroCos furthest away from the heated HTS CroCo #2 are shown as indistinguishable light grey lines only. Few seconds after heater activation, the connector voltages of HTS CroCo #2 drops to ~40% and increases after a short spike to ~0.65 mV. At cable currents substantially smaller than the critical current, the voltage on the connectors can be considered as an estimate of the individual currents. As the total cable current is constant, current has to redistribute to other strands. In fact, an increase of the normalized voltages of the connectors for all other HTS CroCo strands is observed. In particular for the neighboring HTS CroCos #1 and #5, denoted by black and grey squares, respectively, an initial voltage spike is found. For the next-neighboring HTS CroCos (black/grey circles) a steep slope (but no peak) is found. These observations show that current is redistributed to the other HTS CroCos, the closer the HTS CroCos, the faster the initial redistribution. Due to the ring-shaped connector geometry (see Fig. 2(c) and (d)) and the 10 cm deep soldered connector length, the current has to flow around the individual HTS CroCos in order to redistribute to the strands on the opposite side. Therefore, the observed sequential redistribution to neighboring strands first can be explained from the connector geometry.

The measurement was repeated at a cable current of 37.5 kA, i.e., close to I_c. The right column of subfigures in Fig. 5 shows the results. After heater activation at I_{heater} = 0.8 A, the voltage on the terminal decreases to ~40%, but now all HTS CroCos show a voltage beyond the critical current criterion (0.28 mV) as can be seen from Fig. 5(f). Additionally, it was observed that the voltage on negative terminal of HTS CroCo #3 (Fig. 5(b), black triangles) started to increase continuously with time. As the voltage of #3 remained roughly constant on the positive terminal for t < 60 s, one notes that this strand quenches at the negative terminal. During the last seconds before this strand triggered the quench detection system, the voltage on its positive terminal and the superconductor dropped (Fig. 5(d)), i.e. this strand carried less current, which redistributed to the remaining strands leading to a further increase in voltage there.

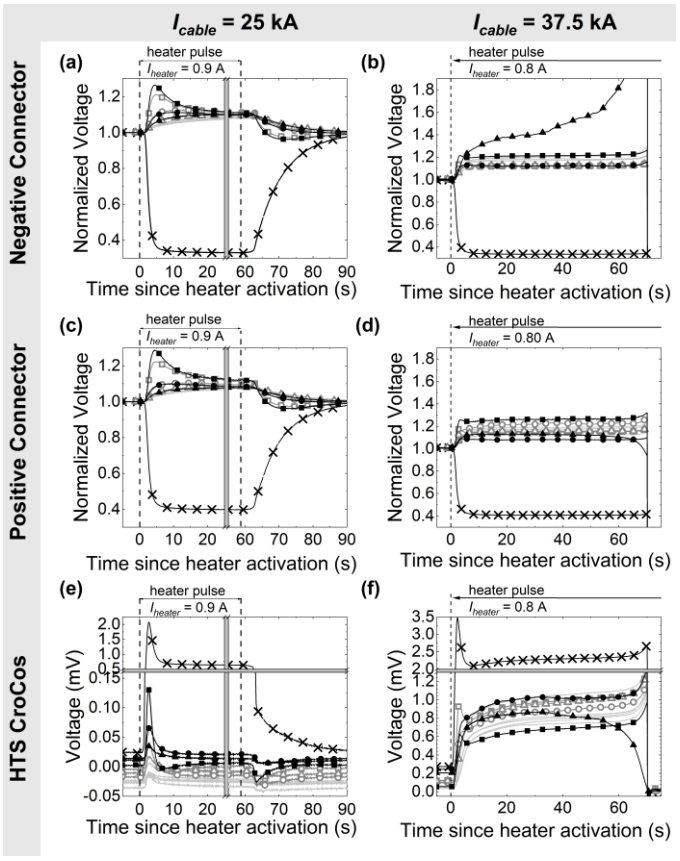

Fig. 5 Response of the demonstrator to heater pulses for two cable currents I_{cable} = 25 kA (left column) and I_{cable} = 37.5 kA (right column).
Top row (a) and (b): Normalized voltage of the negative connector, i.e. $V_{c-}(t) / V_{c-}(t<0)$, as function of time. Center row (c) and (d): Normalized voltage of the positive connector, i.e. $V_{c+}(t) / V_{c+}(t<0)$, as function of time. Bottom row (e) and (f): Voltage long the 2.8 m long mid-sections of the HTS CroCos.
Note that the axes of subfigures (a), (c), (e), (f) are split as denoted by the grey bars and that the vertical axis scales are different for the two parts of (e) and (f). The five HTS CroCos furthest away from the heated HTS CroCo #2 are shown as indistinguishable light grey lines only.

VI. Conclusion and Outlook

The introduction of common connectors to the ends of the twelve HTS CroCo strands of a HTS high current demonstrator led to a noticeable improvement of the demonstrator's electrical performance. Compared to previous work (without common connector) the critical current increased from 33 kA to 37.6 kA and the current range in which all twelve HTS CroCos reached the critical voltage from >7 kA to 2 kA. The results can be well described by a simple electric circuit model, from which the contact resistances from 325 nΩ to 548 nΩ for both connections could be extracted.

An electric heater was installed on one of the twelve CroCos and activated at fixed current to investigate current redistribution through the newly introduced common connector at different cable currents. The voltages on the terminals were used as an estimate of the current in the individual strands. Current redistributes first to the neighboring strands then along the circular arrangement to HTS CroCos further away. At critical currents close to the cable critical current, the activation of the heater triggered a quench of the cable at the terminal of a non-heated strand.

The separable common connector concept will be used in further work on HTS multi-strand cable investigations, in which other aspects towards the realization of HTS high-current DC cables will be investigated in detail.

REFERENCES

[1] H. Kvande and P. A. Drabløs, "The Aluminum Smelting Process and Innovative Alternative Technologies," *Journal of Occupational and Environmental Medicine*, vol. 56, pp. S23-S32, May 2014.

[2] A. Morandi, "HTS dc transmission and distribution: concepts, applications and benefits," *Superconductor Science and Technology*, vol. 28, Art. ID.123001, 2015.

[3] M. Runde, "Application of High-Tc superconductors in Aluminum Electrolysis Plants," *IEEE Trans. Appl. Supercond.*, vol. 5, no. 2, pp. 813-816, June 1995.

[4] F. Schreiner, *et al*., "Design and Manufacturing of a Multistage Cooled Current Lead for Superconducting High Current DC Busbars in Industrial Applications," *IEEE Trans. Appl. Supercond.*, vol. 27, no. 4, Art. ID. 4802405, June 2017.

[5] A. Preuß, "Development of high temperature superconductor cables for large current applications", KIT Scientific publishing, Karlsruhe, Germany: in press.

[6] D. Zhang *et al*., "Stability Analysis of the Cable Core of a 10 kA HTS DC Power Cable Used in the Electrolytic Aluminum Industry," *IEEE Trans. Appl. Supercond.*, vol. 25, no. 3, Art. ID. 5402304, June 2015.

[7] M. Tomita, M. Muralidhar, K. Suzuki, Y. Fukumoto and A. Ishiara, "Development of 10 kA high temperature superconducting power cable for railway systems," *J. Appl. Phys.*, vol. 111, no. 6, Art. ID. 063910, 2012.

[8] S. Elschner, *et al.*, "3S–Superconducting DC-Busbar for High Current Applications," *IEEE Trans. Appl. Supercond.*, vol. 28, no. 4, Art. ID. 4800805, 2018.

[9] A. Preuss, M. J. Wolf, M. Heiduk, C. Lange and W. Fietz, "Production and Characterization of Strands for a 35 kA HTS DC Cable Demonstrator," *IEEE Trans. Appl. Supercond.*, vol. 29, no. 5, Art. ID. 5402905, Aug 2019.

[10] K.-P. Weiss, W. H. Fietz, M. Heiduk, C. Lange, A. Preuß and M. J. Wolf, "Development and test of a 35 kA - HTS CroCo cable demonstrator," *Journal of Physics: Conference Series*, vol. 1559, Art. ID. 012082, 2020.

[11] M. J. Wolf *et al.*, "HTS CroCo - a Strand for High Direct Current Applications," *Journal of Physics: Conference Series*, vol. 1590, Art. ID. 012020, 2020.

[12] V. S. Vysotsky, V. Tsikhon und G. Mulder, „Quench development in superconducting cable having insulated strands with high resistive matrix. I. Experiment," *IEEE Transactions on Magnetics*, vol. 28, no. 1, pp. 735 - 738, January 1992.

[13] G. Mulder, L. van de Klundert und V. Vysotsky, „Quench Development in Superconducting Cable Having Insulated Strands With High Resistive Matrix," *IEEE Transactions on Magnetics*, vol. 28, no. 1, pp. 739 - 742, January 1992.

[14] V. Vysotsky, M. Takayasu, P. Michael, J. Schultz, J. Minervini und S. Jeong, „Current distribution in a 12 strand Nb_3Sn CICC and its influence on ramp rate limitation," *IEEE Trans. Appl. Supercond.*, vol. 7, no. 2, pp. 774-777, June 1997.

[15] T. Mulder, A. Dudarev, M. Mentink, D. van der Laan, M. Dhalle und H. ten Kate, „Performance Test of an 8 kA @ 10-T 4.2-K ReBCO-CORC Cable," *IEEE Trans. Appl. Supercond.*, vol. 26, no. 4, Art.ID 4803705, June 2016.